Electron antineutrino search at the Sudbury Neutrino Observatory

B. Aharmim,[5] S. N. Ahmed,[10] E. W. Beier,[9] A. Bellerive,[3] S. D. Biller,[8] J. Boger,[2,a] M. G. Boulay,[7] T. J. Bowles,[7] S. J. Brice,[7,b] T. V. Bullard,[13] Y. D. Chan,[6] M. Chen,[10] X. Chen,[6,c] B. T. Cleveland,[8] G. A. Cox,[13] X. Dai,[3,8] F. Dalnoki-Veress,[3,d] P. J. Doe,[13] R. S. Dosanjh,[3] G. Doucas,[8] M. R. Dragowsky,[7,e] C. A. Duba,[13] F. A. Duncan,[10] M. Dunford,[9] J. A. Dunmore,[8] E. D. Earle,[10] S. R. Elliott,[7] H. C. Evans,[10] G. T. Ewan,[10] J. Farine,[5,3] H. Fergani,[8] F. Fleurot,[5] J. A. Formaggio,[13] M. M. Fowler,[7] K. Frame,[8,3,7] W. Frati,[9] B. G. Fulsom,[10] N. Gagnon,[13,7,6,8] K. Graham,[10] D. R. Grant,[3,e] R. L. Hahn,[2] A. L. Hallin,[10] E. D. Hallman,[5] A. S. Hamer,[7,f] W. B. Handler,[10] C. K. Hargrove,[3] P. J. Harvey,[10] R. Hazama,[13,g] K. M. Heeger,[6] W. J. Heintzelman,[9] J. Heise,[7] R. L. Helmer,[12,1] R. J. Hemingway,[3] A. Hime,[7] M. A. Howe,[13] P. Jagam,[4] N. A. Jelley,[8] J. R. Klein,[14,9] L. L. Kormos,[10] M. S. Kos,[7,10] A. Krüger,[5] C. B. Krauss,[10] A. V. Krumins,[10] T. Kutter,[1,h] C. C. M. Kyba,[9] H. Labranche,[4] R. Lange,[2] J. Law,[4] I. T. Lawson,[4] K. T. Lesko,[6] J. R. Leslie,[10] I. Levine,[3,i] S. Luoma,[5] R. MacLellan,[10] S. Majerus,[8] H. B. Mak,[10] J. Maneira,[10] A. D. Marino,[6] N. McCauley,[9] A. B. McDonald,[10] S. McGee,[13] G. McGregor,[8,b] C. Mifflin,[3] K. K. S. Miknaitis,[13] G. G. Miller,[7] B. A. Moffat,[10] C. W. Nally,[1] M. S. Neubauer,[9,j] B. G. Nickel,[4] A. J. Noble,[10,3,12] E. B. Norman,[6] N. S. Oblath,[13] C. E. Okada,[6] R. W. Ollerhead,[4] J. L. Orrell,[13,k] S. M. Oser,[1,9] C. Ouellet,[10,l] S. J. M. Peeters,[8] A. W. P. Poon,[6] K. Rielage,[13] B. C. Robertson,[10] R. G. H. Robertson,[13] E. Rollin,[3] S. S. E. Rosendahl,[6,m] V. L. Rusu,[9,n] M. H. Schwendener,[5] O. Simard,[3] J. J. Simpson,[4] C. J. Sims,[8] D. Sinclair,[3,12] P. Skensved,[10] M. W. E. Smith,[13] N. Starinsky,[3,o] R. G. Stokstad,[6] L. C. Stonehill,[13] R. Tafirout,[5] Y. Takeuchi,[10] G. Tešić,[3] M. Thomson,[10] T. Tsui,[1] R. Van Berg,[9] R. G. Van de Water,[7] C. J. Virtue,[5] B. L. Wall,[13] D. Waller,[3] C. E. Waltham,[1] H. Wan Chan Tseung,[8] D. L. Wark,[11] N. West,[8] J. B. Wilhelmy,[7] J. F. Wilkerson,[13] J. R. Wilson,[8] P. Wittich,[9] J. M. Wouters,[7] M. Yeh,[2] and K. Zuber[8]

(SNO Collaboration)

[1]*Department of Physics and Astronomy, University of British Columbia, Vancouver, British Columbia V6T 1Z1 Canada*
[2]*Chemistry Department, Brookhaven National Laboratory, Upton, New York 11973-5000, USA*
[3]*Ottawa-Carleton Institute for Physics, Department of Physics, Carleton University, Ottawa, Ontario K1S 5B6 Canada*
[4]*Physics Department, University of Guelph, Guelph, Ontario N1G 2W1 Canada*
[5]*Department of Physics and Astronomy, Laurentian University, Sudbury, Ontario P3E 2C6 Canada*
[6]*Institute for Nuclear and Particle Astrophysics and Nuclear Science Division, Lawrence Berkeley National Laboratory, Berkeley, California 94720, USA*
[7]*Los Alamos National Laboratory, Los Alamos, New Mexico 87545, USA*
[8]*Department of Physics, University of Oxford, Denys Wilkinson Building, Keble Road, Oxford, OX1 3RH, United Kingdom*
[9]*Department of Physics and Astronomy, University of Pennsylvania, Philadelphia, Pennsylvania 19104-6396, USA*
[10]*Department of Physics, Queen's University, Kingston, Ontario K7L 3N6 Canada*
[11]*Rutherford Appleton Laboratory, Chilton, Didcot, Oxon, OX11 0QX, United Kingdom and University of Sussex, Physics and Astronomy Department, Brighton BN1 9QH, United Kingdom*
[12]*TRIUMF, 4004 Wesbrook Mall, Vancouver, BC V6T 2A3, Canada*
[13]*Center for Experimental Nuclear Physics and Astrophysics and Department of Physics, University of Washington, Seattle, Washington 98195, USA*
[14]*Department of Physics, University of Texas at Austin, Austin, Texas 78712-0264, USA*
(Received 15 July 2004; published 29 November 2004)

[a]Present address: U.S. Department of Energy, Germantown, Maryland, USA
[b]Present address: Fermilab, Batavia, Illinois, USA
[c]Present address: Stanford Linear Accelerator Center, Menlo Park, California, USA
[d]Present address: Max-Planck-Institut for Nuclear Physics, Heidelberg, Germany
[e]Present address: Department of Physics, Case Western Reserve University, Cleveland, Ohio, USA
[f]Deceased
[g]Present address: Research Center for Nuclear Physics and Osaka University, Osaka, Japan
[h]Present address: Department of Physics and Astronomy, Louisiana State University, Baton Rouge, Louisiana, USA
[i]Present address: Department of Physics and Astronomy, Indiana University, South Bend, Indiana, USA
[j]Present address: Department of Physics, University of California at San Diego, La Jolla, California, USA
[k]Present address: Pacific Northwest National Laboratory, Richland, Washington, USA
[l]Present address: Department of Physics, McMaster University, Hamilton, Ontario, Canada
[m]Present address: Lund University, Sweden
[n]Present address: Department of Physics, University of Chicago, Chicago, Illinois, USA
[o]Present address: René J. A. Lévesque Laboratory, Université de Montréal, Montreal, Quebec City, Canada

Upper limits on the $\bar{\nu}_e$ flux at the Sudbury Neutrino Observatory have been set based on the $\bar{\nu}_e$ charged-current reaction on deuterium. The reaction produces a positron and two neutrons in coincidence. This distinctive signature allows a search with very low background for $\bar{\nu}_e$'s from the Sun and other potential sources. Both differential and integral limits on the $\bar{\nu}_e$ flux have been placed in the energy range from 4–14.8 MeV. For an energy-independent $\nu_e \rightarrow \bar{\nu}_e$ conversion mechanism, the integral limit on the flux of solar $\bar{\nu}_e$'s in the energy range from 4–14.8 MeV is found to be $\Phi_{\bar{\nu}_e} \leq 3.4 \times 10^4$ cm^{-2} s^{-1} (90% C.L.), which corresponds to 0.81% of the standard solar model ^{8}B ν_e flux of 5.05×10^6 cm^{-2} s^{-1}, and is consistent with the more sensitive limit from KamLAND in the 8.3–14.8 MeV range of 3.7×10^2 cm^{-2} s^{-1} (90% C.L.). In the energy range from 4–8 MeV, a search for $\bar{\nu}_e$'s is conducted using coincidences in which only the two neutrons are detected. Assuming a $\bar{\nu}_e$ spectrum for the neutron induced fission of naturally occurring elements, a flux limit of $\Phi_{\bar{\nu}_e} \leq 2.0 \times 10^6$ cm^{-2} s^{-1} (90% C.L.) is obtained.

DOI: 10.1103/PhysRevD.70.093014 PACS numbers: 14.60.St, 13.15.+g, 13.35.Hb

I. INTRODUCTION

This paper presents results from a search for $\bar{\nu}_e$'s with the Sudbury Neutrino Observatory (SNO) via the charged-current reaction ($\overline{\text{CC}}$) on deuterons:

$$\bar{\nu}_e + d \rightarrow e^+ + n + n - 4.03 \text{ MeV}.$$

The distinctive signature of a positron in coincidence with two neutrons allows SNO to search for $\bar{\nu}_e$'s with very low background. By means of (n, n)-coincidence detections, SNO has sensitivity to $\bar{\nu}_e$'s with energies above the reaction threshold of 4.03 MeV. For coincidences involving a e^+, SNO is sensitive to $\bar{\nu}_e$'s above a threshold of 4 MeV + $E^{\text{thr}}_{\text{recoil}}$, where $E^{\text{thr}}_{\text{recoil}}$ is the analysis threshold applied to the recoil positron. We present results for integral $\bar{\nu}_e$ flux limits in the neutrino energy range from 4–14.8 MeV under the assumption that $\bar{\nu}_e$'s originate from a ^{8}B spectrum and below 8 MeV under the assumption that $\bar{\nu}_e$'s originate from a fission spectrum. Differential limits on the $\bar{\nu}_e$ flux have been placed, independent of any particular spectral assumptions.

As a solution to the solar neutrino problem [1], analyses of global solar neutrino data favor matter-enhanced neutrino oscillations with mixing parameters in the large mixing angle (LMA) region [2,3]. Studies of solar neutrino data have demonstrated that approximately two-thirds of ^{8}B solar neutrinos convert to active flavors other than ν_e before reaching Earth [2,4–8]. The deficit of reactor antineutrinos reported by the Kamioka Liquid scintillator Anti-Neutrino Detector (KamLAND) experiment [7] supports the LMA solution to the solar neutrino problem under the explicit assumption of CPT conservation in the neutrino sector. More generally the spin flavor precession (SFP) mechanism [9,10] or neutrino decay [11] could contribute to the observed neutrino flavor transformation at a subdominant level by converting a small fraction of solar ν_e to $\bar{\nu}_e$. In SFP models, neutrinos are assumed to have a transition magnetic moment of the order of 10^{-11} Bohr magnetons [10] if they are of Majorana type. Solar magnetic fields, which are known to be time dependent, couple to this magnetic moment to convert ν_e into $\bar{\nu}_e$ with a combination of neutrino flavor oscillations and SFP mechanisms. Neutrino decay models allow heavier neutrino mass eigenstates to decay into light $\bar{\nu}$ [11].

Nuclear fission $\bar{\nu}_e$ spectra peak at low energies and fall approximately exponentially with energy and have negligible intensity above 8 MeV [12]. Positrons produced in $\overline{\text{CC}}$ reactions from fission $\bar{\nu}_e$'s are too low in energy to be detected by the present $\bar{\nu}_e$ analysis. However, by conducting an analysis involving only (n, n)-coincidences it is possible to study the energy region from 4–8 MeV, providing some sensitivity to $\bar{\nu}_e$'s that might originate from naturally occurring neutron induced fission sources. Because the fission spectrum is significant in this energy region, whereas the ^{8}B spectrum is peaked at higher energies, a separate analysis of this region for $\bar{\nu}_e$'s originating from fission is performed. The expected flux from man-made reactors would provide a negligible contribution to this analysis.

Additional sources of $\bar{\nu}_e$'s are cosmic ray interactions in the upper atmosphere and the diffuse supernovae background. The flux of these types of $\bar{\nu}_e$'s are dominated by $\bar{\nu}_e$ energies above the 4–14.8 MeV energy range investigated in the present analysis and hence are only addressed peripherally by the differential limits below 15 MeV.

II. EXPERIMENTAL DATA

SNO is an imaging water Cherenkov detector located at a depth of 6010 m of water equivalent in the Inco, Ltd. Creighton mine near Sudbury, Ontario, Canada. SNO detects neutrinos using an ultrapure heavy water target contained in a transparent acrylic spherical shell 12 m in diameter. Cherenkov photons generated in the heavy water are detected by 9456 photomultiplier tubes (PMTs) mounted on a stainless steel geodesic sphere 17.8 m in diameter. The geodesic sphere is immersed in ultrapure light water to provide shielding from radioactivity in both the PMT array and the cavity rock. The SNO detector has been described in detail in [13].

The data reported here were recorded between November 2, 1999, and May 28, 2001, and span the entire first phase of the experiment, in which only D_2O was

present in the sensitive volume. In comparison to earlier SNO analyses [5,6], a cut employed to remove events following muon candidates was modified to maximize rejection of false $\bar{\nu}_e$ candidates. Any event with an assigned kinetic energy above 18 MeV and all events following that event within 0.5 s are rejected. These modifications resulted in a total live time of 305.9 live days, a reduction of less than 0.2% from SNO's neutral-current (NC) analysis [6].

III. ANALYSIS

Interactions of $\bar{\nu}_e$'s with deuterons produce a positron and two neutrons. The positron generates a prompt Cherenkov signal, while the neutrons must first thermalize before generating 6.25 MeV gamma rays from their capture on deuterons. The mean neutron capture time is 42 ms and the diffusion length is $\sim$110 cm in pure D_2O. Inside the D_2O volume $\bar{\nu}_e$ events can be identified by a coincidence of two or three particles.

The analysis procedure consists of two steps. The first is similar to the SNO solar neutrino analysis and is described in [6]. In this step, PMT times and hit patterns are used to reconstruct event vertices and assign to each recoil positron or electron a most probable kinetic energy, $T_{\rm eff}$. The recoil threshold in this analysis was $T_{\rm eff} \geq 5$ MeV, providing sensitivity to positrons and neutrons from the $\overline{\rm CC}$ reaction. No $\bar{\nu}_e$'s originating from the conversion of solar ν_e's are expected to have energies in excess of 14.8 MeV. Hence, the 18 MeV upper limit on recoil positron or electron energy does not remove potential solar or fission $\bar{\nu}_e$ candidates. A fiducial volume was defined by requiring reconstructed event vertices to be within 550 cm of the center of the acrylic vessel. This reduces both the number of externally produced background events and the systematic uncertainties associated with optics and event reconstruction near the acrylic vessel.

The second step of the analysis identifies coincidences among the accepted events. The size of the coincidence window, chosen to be 150 ms, was optimized to maximize the sensitivity to 2-fold coincidences in the presence of the background of accidental coincidences. Antineutrino candidates that are part of a burst of four or more e^+ or n-like events of any energy are discarded. Even under the assumption that 100% of the solar ν_e are converted to $\bar{\nu}_e$'s, four- or higher-fold coincidences are 10^3 times more likely to originate from a background such as atmospheric ν's or spontaneous fission of ^{238}U than from a 3-fold $\bar{\nu}_e$ event in coincidence with a random event, as determined by Monte Carlo simulations.

A. Detection Efficiencies

Coincidence detection efficiencies were determined from a simulated $\bar{\nu}_e$ data set. The Monte Carlo (MC) simulations sampled $\bar{\nu}_e$'s from a ^{8}B energy spectrum [14] with a total flux 100 times the standard solar model (SSM-BP00) ^{8}B flux [15]. The simulated data set matches the experimentally recorded data set in duration and correctly describes the detector status as a function of time. Based on the number of simulated $\bar{\nu}_e$ interactions inside the D_2O volume and extracted coincidences inside the signal region, the 2- and 3-fold coincidence event detection efficiencies were found to be

$$\epsilon_{(e^+,n,n)} = 1.11 \pm 0.02(\text{stat})^{+0.05}_{-0.12}(\text{syst})\%,$$
$$\epsilon_{(e^+,n)} = 10.27 \pm 0.05(\text{stat})^{+0.37}_{-0.94}(\text{syst})\%,$$
$$\epsilon_{(n,n)} = 1.20 \pm 0.02(\text{stat})^{+0.05}_{-0.10}(\text{syst})\%.$$

The systematic uncertainties were derived by comparing the number of reconstructed coincidences with the true number of coincidences within the fiducial volume and energy region of the analysis. Among coincidences originating from $\bar{\nu}_e$ interactions, (e^+, n)-coincidences are 10 times more likely to be detected than (n, n)-coincidences or (e^+, n, n)-coincidences. While the (n, n)-coincidences can originate from $\bar{\nu}_e$'s with energies as low as 4 MeV, coincidences containing a positron must originate from $\bar{\nu}_e$'s with energies above 9 MeV. Figure 1 displays the number of expected $\bar{\nu}_e$ events as function of the antineutrino energy under the assumption that $\bar{\nu}_e$'s originate from a ^{8}B spectrum with a total flux of 5.05×10^6 cm^{-2} s^{-1}. The above coincidence detection efficiencies are consistent with the average e^+ detection efficiency estimated from Monte Carlo $\overline{\epsilon}_{e^+} = 40.09^{+1.50}_{-4.62}(\text{syst}) \pm 0.10(\text{stat})\%$ and an average neutron detection efficiency of $\overline{\epsilon}_n = 14.38 \pm 0.53\%$ [6]. The neutron response and systematic uncertainty on the response were calibrated with a ^{252}Cf source.

B. Backgrounds

Backgrounds to the $\bar{\nu}_e$ search can be divided into two categories: coincidences caused by $\bar{\nu}_e$'s from known sources and coincidences from processes other than $\bar{\nu}_e$ charged-current reactions. These are presented in Table II. The first category has contributions from atmospheric, reactor, and diffuse supernovae $\bar{\nu}_e$'s. The background contribution from atmospheric $\bar{\nu}_e$'s is estimated to be 0.07 ± 0.01 coincidences. It is derived from the $\overline{\rm CC}$ cross sections [16], coincidence detection efficiencies, and a parameterized $\bar{\nu}_e$ spectrum extrapolated into the energy range below 50 MeV [17]. Highly energetic atmospheric $\bar{\nu}_e$'s only contribute to the background if detected as (n, n)-coincidences, due to the applied upper bound on the recoil lepton energy. The background estimate from nuclear power reactors yields 0.019 ± 0.002 coincidences. The calculation is based on the monthly reported actual power output of all commercial reactors [18] within 500 km of SNO and an average reactor $\bar{\nu}_e$ spectrum [12,19]. Furthermore, the $\bar{\nu}_e$ flux is assumed to be reduced as a result of neutrino oscillations governed by the

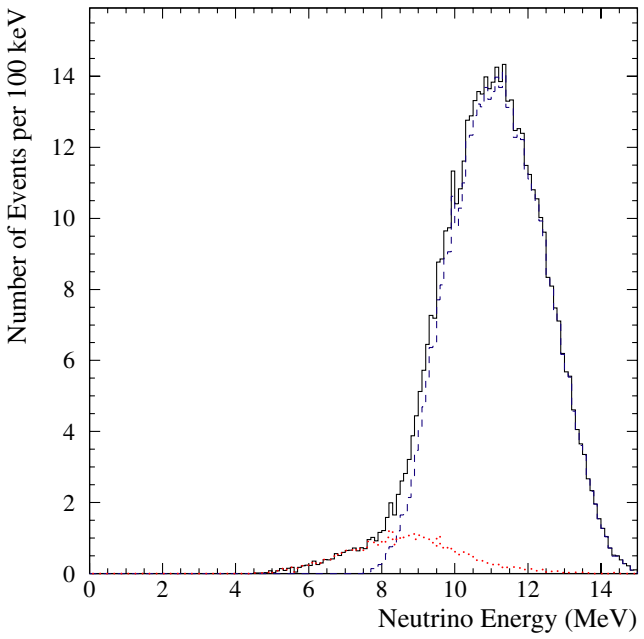

FIG. 1 (color online). Number of expected coincidence events as a function of the antineutrino energy, for $\bar{\nu}_e$'s originating from a ^{8}B spectrum with a total flux of 5.05×10^6 cm^{-2} s^{-1}. Coincidences containing a positron and (n, n)-coincidences are shown as dashed and dotted histograms, respectively. The solid line represents all types of detected coincidences as a function of $\bar{\nu}_e$ energy.

best fit oscillation parameters $\tan^2(\theta) = 0.41$ and $\Delta m^2 = 7.1 \times 10^{-5}$ eV^2 [8]. The number of $\overline{\text{CC}}$ interactions from diffuse supernovae neutrinos was estimated by combining a theoretical flux calculation [20] with SNO's detection efficiency and contributes ≤ 0.005 coincidences. The calculation is consistent with experimental limits [21]. Electron antineutrinos from the decay chain of terrestrial radioisotopes such as ^{238}U and ^{232}Th, geo-antineutrinos, do not contribute to the background because their energies are below the threshold of the $\overline{\text{CC}}$ reaction.

The main contributions to the second category of backgrounds originate from atmospheric ν, possible ^{238}U fission events in the detector media, and accidental coincidences. The atmospheric ν background is estimated to account for $1.46^{+0.49}_{-0.45}$ coincidences. Atmospheric neutrinos were sampled from a realistic spectrum [17] and propagated with the neutrino-interaction generator NUANCE [22]. Detailed event information, including energy and multiplicities at the depth of SNO, was then processed by a full detector simulation. The uncertainty on the atmospheric ν background is a combination of effects associated with the performance of the detector and the detector MC simulation, particle interactions as simulated by NUANCE, and the uncertainty in the primary cosmic ray (CR) flux. The dominant contributions are the normalization of the primary CR flux and the Pauli suppression. Table I details these and other major contributions to the total rate uncertainty.

Spontaneous fission background from ^{238}U in detector media was estimated to contribute less than 0.79 coincidences. This limit was derived from an inductively coupled plasma mass spectrometer (ICP-MS) measurement of the ^{238}U concentration of 66 ± 17 (fg U)/g D_2O) [23], for which approximately 14 spontaneous fission decays of ^{238}U are expected per kton-year. The detector response was calculated on the basis of detection efficiencies and a discrete probability distribution for neutron multiplicities in spontaneous fission [24]. The ICP-MS measurement is consistent with a statistically limited multiplicity measurement of the data. The above estimate is an upper limit since the ICP-MS measurement did not include procedural blanks, and the ^{238}U concentration measurement was obtained on September 4, 2003, after the data set reported here, and after the addition of NaCl to the heavy water. Because the reverse osmosis purification system, which was operated while the data accumulated for the present analysis, could not be run with NaCl in the heavy water, the measurement is likely to include more ^{238}U contamination than was present when the data were taken.

Accidental coincidences are formed by individual events that pass the analysis cuts and have a random time correlation. Their number has been calculated as a function of the time-dependent singles rate in the detector and amounts to $0.13^{+0.06}_{-0.04}$ coincidences. This number was confirmed independently by a direct measurement of signals following within 150 ms of a large number of random triggers.

The background from neutron capture reactions on oxygen, which can produce multiple gamma rays above

TABLE I. The dominant contribution to the uncertainty on the background originating from atmospheric neutrinos. The total uncertainties for the charged-current (CC) and neutral-current interactions are derived from Monte Carlo simulations. The NC interaction rate is unaffected by changes in the neutrino mixing parameters for active neutrino species.

Parameter	CC rate(%)	NC rate (%)
θ_{12}	$^{+1.5}_{-5.9}$	N/A
Δm^2_{12}	$^{+1.3}_{-0.0}$	N/A
θ_{23}	$^{+4.4}_{-0.0}$	N/A
Δm^2_{23}	$^{+2.1}_{-1.3}$	N/A
Axial Mass	$^{+9.2}_{-6.4}$	$^{+9.2}_{-9.4}$
Pauli Suppression	$^{+14.4}_{-15.4}$	$^{+19.4}_{-19.2}$
Resonance Uncertainty	± 6.8	± 7.3
Primary CR Flux	± 20.0	± 20.0
Total	$^{+27.7}_{-27.6}$	$^{+30.2}_{-30.2}$

TABLE II. Types of coincidence backgrounds and number of expected coincidences in the SNO detector for the data set. Upper limits and uncertainties on individual backgrounds have been combined under the assumption that they are independent.

$\bar{\nu}_e$ background	
Type of $\bar{\nu}_e$	expected coincidences
Atmospheric	0.07 ± 0.01
Reactor	0.019 ± 0.002
Diffuse supernovae	≤ 0.005
Geo-antineutrinos	0.0
Total $\bar{\nu}_e$'s background	0.09 ± 0.01
Non-$\bar{\nu}_e$ background	
Process	expected coincidences
Atmospheric ν	$1.46\,^{+0.49}_{-0.45}$
^{238}U spontaneous fission in detector media	<0.79
Accidental coincidences	$0.13\,^{+0.06}_{-0.04}$
^{x}O(n, γ)$^{x+1}$O, where x = 17, 18	<0.05
Instrumental contamination (95% C.L.)	<0.027
^{13}C(α, ne^+e^-)^{16}O (90% C.L.)	$<1.7 \times 10^{-3}$
Intrinsic:	
^{214}Bi:$\beta - \gamma$ decay	7.6×10^{-5}
^{210}Tl:$\beta - n$ decay	$\approx 10^{-8}$
^{208}Tl:$\beta - \gamma$ decay	8.7×10^{-4}
$\gamma \rightarrow$ Compton e^- + photo-disintegration n	$<8 \times 10^{-4}$
Total non-$\bar{\nu}_e$ background	$1.59\,^{+0.93}_{-0.45}$
Total background	$1.68\,^{+0.93}_{-0.45}$

the deuteron photodisintegration threshold, was estimated to be less than 0.05 coincidences. It was calculated from abundances of ^{17}O and ^{18}O, relative intensities of gamma rays produced in ^{17}O(n, γ)^{18}O and ^{18}O(n, γ)^{19}O reactions, the ratio $P_{^{17}\mathrm{O},^{18}\mathrm{O}}/P_{\mathrm{D}}$ of the neutron capture probability on ^{17}O and ^{18}O and deuterium, as well as the total number of observed neutrons. Instrumental backgrounds are events produced by electrical pickup or emission of non-Cherenkov light from detector components. Their background contribution is determined to be <0.027 coincidences (95% C.L.). The number of coincidences of this type is assessed by means of a bifurcated analysis, which employs sets of orthogonal cuts aimed at instrumental background rejection. The background from α-capture reactions on carbon, which can produce a neutron in coincidence with an $e^+ - e^-$ pair, was found to be less than 1.7×10^{-3} (90% C.L.) coincidences. It was estimated on the basis of the total number of neutrons in the signal region and a MC calculation. Other backgrounds originate from radioisotope contamination and can produce coincidences through $\beta - \gamma$ or $\beta - n$ decays but are found to be entirely negligible. They are estimated on the basis of their respective radioisotope contamination levels.

Upper limits and uncertainties on individual backgrounds have been combined under the assumption that they are independent. The total background amounts to $1.68^{+0.93}_{-0.45}$ coincidences. The uncertainty on the total background is conservative since uncertainties and intervals of different confidence levels (C.L.) have been combined under the assumption that all are at the 68% C.L.

IV. RESULTS

The search for $\bar{\nu}_e$ candidates in the experimental data set employs the same cuts on energy and fiducial volume as well as the same coincidence extraction algorithms as were used to derive the Monte Carlo-based coincidence detection efficiencies. One 3-fold and one 2-fold coincidence were found. Table III summarizes the characteristics of the two $\bar{\nu}_e$ candidate coincidences and their constituent events. On an event-by-event basis it is not possible to uniquely identify individual constituent events as a positron or a neutron. Therefore, the analysis regroups (e^+, n)- and (n, n)-coincidences into a single category of 2-fold coincidences. This category has an order of magnitude higher sensitivity than 3-fold coincidences and is sensitive to $\bar{\nu}_e$'s with energies as low as 4 MeV.

TABLE III. Two $\bar{\nu}_e$ candidate coincidences are found. Listed are kinetic recoil lepton energy and radial position for each constituent event as well as spatial separation and time separation relative to the first particle in each coincidence.

$\bar{\nu}_e$ candidate		$T_{\rm eff}$ (MeV)	$r_{\rm fit}$ (cm)	Δr (cm)	Δt (ms)
I	1st particle	8.58	283.2	0.0	0.0
	2nd particle	5.39	472.4	206.7	16.7
	3rd particle	5.15	349.2	178.3	20.3
II	1st particle	6.95	506.4	0.0	0.0
	2nd particle	6.09	429.5	81.8	88.9

A. Differential Limits

This analysis sets model-independent differential limits on the $\bar{\nu}_e$ flux in the neutrino energy range from 4–14.8 MeV. Bin sizes in neutrino energy were chosen to be 1 MeV. Based on the observed 2-fold coincidence, and under the conservative assumption of zero background, the Bayesian upper limit [25] on the number of 2-fold coincidences amounts to 3.89 at the 90% C.L. In each neutrino energy bin, it is assumed that the candidate 2-fold event was produced by an $\bar{\nu}_e$ of that energy. The upper limit on the number of candidate events is then corrected for detector acceptance and cross section to obtain a limit on the absolute $\bar{\nu}_e$ flux at that energy. As a result, the limit in each energy bin is model-independent and maximally conservative, but limits in different energy bins are strongly correlated. Systematic uncertainties in the theoretical cross sections, energy resolution differences between data and MC, simulation failures, as well as systematics related to data reduction combine to about 2% and have been taken into account. Only biases between the data and the Monte Carlo are important to derive a flux limit and therefore the quoted uncertainty for the detection efficiency cannot be counted in full. Simulation failures are mostly signal or background events for which the MC was not able to successfully track all Cherenkov photons. Figure 2 displays $\bar{\nu}_e$ flux limits for the energy range from 4–15 MeV at greater than 90% C.L. Super-Kamiokande's (SK) flux limits for monoenergetic $\bar{\nu}_e$'s are shown for comparison [26]. Super-Kamiokande's limits are based on data events, after subtraction of spallation background, which fall in the $\pm 1\sigma$ range of a Gaussian that describes the detector response to monoenergetic $\bar{\nu}_e$'s. The SNO and SK limits are slightly different in nature since SNO limits were calculated for a series of 1 MeV wide bins in neutrino energy.

B. Integral Limit

Under the assumption that the energy distribution of solar $\bar{\nu}_e$'s follows a ^{8}B spectrum, and that both observed candidates are of solar origin, an integral limit on the solar $\bar{\nu}_e$ flux is derived. The 2- and 3-fold coincidences are joined in order to maximize the sensitivity. Using an extended Feldman-Cousins method [27,28] to include the background uncertainty in the form of a two unequal-sided Gaussian, the 90% C.L. upper limit for two candidate coincidences and $1.68^{+0.93}_{-0.45}$ background events has been calculated to be 3.8 coincidences. A MC calculation was used to convert a given $\bar{\nu}_e$ flux into a number of observed events. The 3.8 coincidences translate into a $\bar{\nu}_e$ flux limit of $\Phi < 3.4 \times 10^4$ cm^{-2} s^{-1} in the energy range from 4–14.8 MeV. The systematic uncertainties have been treated similarly to the differential analysis. The analysis energy window contains 83.4% of the SSM-BP00 ^{8}B ν_e flux of $5.05^{+1.01}_{-0.81} \times 10^6$ cm^{-2} s^{-1} [15]. The above limit implies a 90% C.L. upper bound on the conversion probability of solar ^{8}B ν_e's into $\bar{\nu}_e$'s of 0.81%, if $\bar{\nu}_e$'s are assumed to follow a ^{8}B spectrum. This assumption is equivalent to an energy-independent $\nu_e \rightarrow \overline{\nu}_e$ conversion mechanism.

If the analysis is restricted to the $\bar{\nu}_e$ energy range from 4–8 MeV, only the observed 2-fold coincidence represents a $\bar{\nu}_e$ candidate since the 3-fold coincidence could only have originated from a $\bar{\nu}_e$ with an energy in excess of 12.6 MeV. Within the 4–8 MeV energy window the background is conservatively assumed to be zero coincidences. Using a Bayesian prescription [25], the 90% C.L. upper limit on one candidate and zero assumed background corresponds to 3.89 events. Assuming a fission spectral shape [12,19] from possible naturally occurring elements, this defines a limit of $\Phi < 2.0 \times 10^6$ cm^{-2} s^{-1} in the

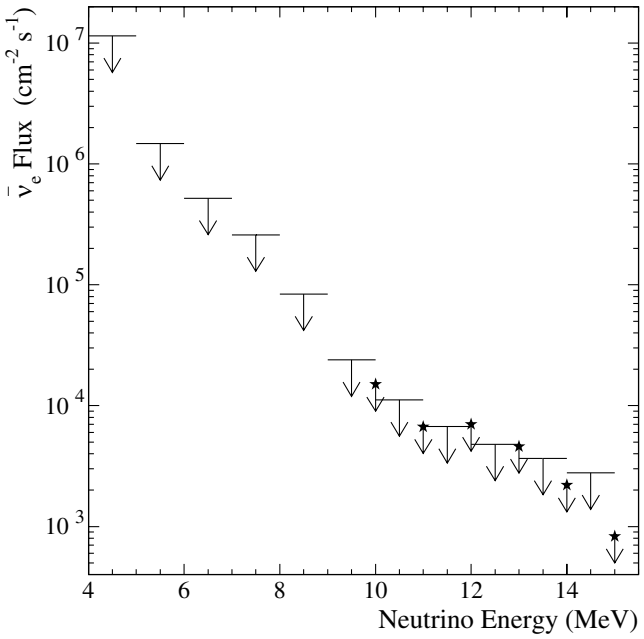

FIG. 2. Limits on the $\bar{\nu}_e$ flux from SNO (bars) and SK (stars). Bars represent 90% C.L. flux limits for 1 MeV wide energy bins and are based on the assumption that the observed 2-fold coincidence originates from that particular energy bin. Stars indicate limits for monoenergetic $\bar{\nu}_e$'s .

energy range from 4–8 MeV which covers 9% of the average reactor $\bar{\nu}_e$ flux.

C. Comparison With Other Experiments

Previously, other experiments have set very stringent limits on the $\bar{\nu}_e$ flux from the Sun. Under the assumption of an unoscillated ^{8}B spectral shape for s olar $\bar{\nu}_e$'s KamLAND [29] limits the solar flux of $\bar{\nu}_e$'s to less than 3.7×10^2 cm^{-2} s^{-1} (90% C.L.). This measurement is based on the neutrino energy range from 8.3–14.8 MeV and corresponds to an upper limit on the $\nu_e \rightarrow \bar{\nu}_e$ conversion probability of 2.8×10^{-4} (90% C.L.).

SK's integral flux limit is based on the energy range from 8–20 MeV and, under the assumption of a ^{8}B spectrum for solar $\bar{\nu}_e$'s and a total $\bar{\nu}_e$ flux of 5.05×10^6 cm^{-2} s^{-1}, places a 90% C.L. limit on the conversion probability of less than 0.8% [26]. This corresponds to an absolute flux limit of 1.4×10^4 cm^{-2} s^{-1} in the energy region from 8–20 MeV which contains 34.4% of the total ^{8}B flux. The present SNO analysis investigates the energy range from 4–14.8 MeV and uses a completely independent direct counting method with very low background. Therefore it can set a comparable limit on the $\bar{\nu}_e$ flux despite the fact that SK's exposure is 800 times larger. Because of the time dependence of the solar magnetic field the $\bar{\nu}_e$ flux originating from conversion of solar ^{8}B neutrinos could vary as function of time. Table IV specifies the existing limits on the $\bar{\nu}_e$ flux and indicates the time frames during which the relevant data were recorded.

The present analysis provides a 90% C.L. upper limit for $\bar{\nu}_e$ energies from 4–8 MeV of 2.0×10^6 cm^{-2} s^{-1} assuming a neutron induced fission spectral shape. Because the contribution from man-made reactors in the region of the SNO detector is calculated to be very low (see Table II) this can be considered as an upper limit on the flux from naturally occurring neutron induced fission sources. However, we note that if all 54 events observed by KamLAND [7] for $\bar{\nu}_e$ energies from 3.4–8 MeV were considered to originate from the neutron induced fission of naturally occurring elements rather than from nearby man-made reactors, an upper limit on the $\bar{\nu}_e$ flux in the 3.4–8 MeV energy region of 1.55×10^5 cm^{-2} s^{-1} (90% C.L.) can be derived for the KamLAND location. During the completion of this paper, KamLAND [7] reported a new result of 258 events in a 515-day live time and a 33% larger fiducial volume. No significant change in the $\bar{\nu}_e$ flux limit is expected as a result.

The neutron detection efficiency in pure D_2O was 14.4% [6]. For the phase of the SNO experiment in which NaCl was added to the D_2O, improving the neutron detection efficiency to 39.9% [8], an increase in the effective $\bar{\nu}_e$ sensitivity by a factor of about three is anticipated.

D. Neutrino Decay

Although flavor transformation of solar neutrinos is believed to be dominated by matter-enhanced neutrino oscillations with mixing parameters in the LMA region, SFP mechanisms or neutrino decay may also contribute. Since neutrino decay is expected to be energy-dependent, SNO's low $\bar{\nu}_e$ energy threshold of 4 MeV is a valuable feature to test for nonradiative neutrino decay of the form $\nu_2 \rightarrow \bar{\nu}_1 + X$. Here ν_2 and ν_1 refer to the heavier and lighter neutrino mass eigenstates and X is a scalar particle (e.g., a Majoron) [11]. For quasidegenerate neutrino masses, a lower limit on the lifetime τ_2 of the heavier neutrino is found to be $\tau_2/m_2 > 0.004$ s/eV. For hierarchical neutrino masses, the limit amounts to $\tau_2/m_2 > 4.4 \times 10^{-5}$ s/eV, equivalent to $\tau_2 > 0.44$ μs if $m_2 \approx 0.01$ eV [32]. Previously, KamLAND [29] has presented lower limits on nonradiative neutrino decay based on the $\bar{\nu}_e$ energy range from 8.3–14.8 MeV and found $\tau_2/m_2 > 0.067$ s/eV for quasidegenerate and $\tau_2 > 11$ μs for hierarchical neutrino masses.

V. CONCLUSION

In summary, our analysis represents a novel detection technique to search for $\bar{\nu}_e$'s, with very low backgrounds. Based on the one 2-fold and one 3-fold observed coincidence, integral limits on the $\bar{\nu}_e$ flux in the energy range below 8 MeV and in the range from 4–14.8 MeV have been set under the assumption of a fission and a ^{8}B spectrum, respectively. Spectrally independent differential limits have been placed as well. The derived limit on the flux of solar $\bar{\nu}_e$'s was used to constrain the

TABLE IV. Integral $\bar{\nu}_e$ flux limits $\bar{\nu}_e$/SSM ν_e at the 90% C.L. relative to the SSM-BP00 ^{8}B flux [15], periods of time during which the relevant data were taken, and energy ranges over which the various experiments have sensitivity to solar $\bar{\nu}_e$ are presented.

Experiment	Time Period	Energy (MeV)	Limit (%)
KamLAND [29]	3/4/2002–12/1/2002	8.3–14.8	0.028
SNO	11/2/1999–5/28/2001	4.0–14.8	0.81
SK [26]	5/31/1996–7/15/2001	8.0–20.0	0.8
LSD [30]	before 4/1996	8.8–18.8	1.95
Kamiokande [31]	6/1988–4/1990	12.0–13.0	5.07

neutrino lifetime. Within SNO's sensitivity we independently confirm the SK and KamLAND results on $\bar{\nu}_e$ fluxes.

ACKNOWLEDGMENTS

This research was supported by the Natural Sciences and Engineering Research Council, Canada; Industry Canada; National Research Council, Canada; Northern Ontario Heritage Fund Corporation, Inco, Canada; Atomic Energy of Canada, Ltd.; Ontario Power Generation; the U.S. Department. of Energy; and Particle Physics and Astronomy Research Council, United Kingdom. We thank the SNO technical staff for their strong contributions.

[1] J. N. Bahcall and R. Davis, Science **191**, 264 (1976).
[2] Q. R. Ahmad *et al.*, Phys. Rev. Lett. **89**, 011 302 (2002).
[3] J. N. Bahcall *et al.*, J. High Energy Phys. 07, (2002) 054; G. L. Fogli *et al.*, Phys. Rev. D **66**, 093008 (2002); V. Barger *et al.*, Phys. Lett. B **537**, 179 (2002).
[4] S. Fukuda *et al.*, Phys. Lett. B **539**, 179 (2002).
[5] Q. R. Ahmad *et al.*, Phys. Rev. Lett. **87**, 071 301 (2001).
[6] Q. R. Ahmad *et al.*, Phys. Rev. Lett. **89**, 011 301 (2002).
[7] K. Eguchi *et al.*, Phys. Rev. Lett. **90**, 021802 (2003); hep-ex/0406035.
[8] S. N. Ahmed *et al.*, Phys. Rev. Lett. **92**, 181 301 (2004).
[9] O. G. Miranda *et al.*, Nucl. Phys. **B595**, 360 (2001); B. C. Chauhan and J. Pulido, Phys. Rev. D **66**, 053006 (2002).
[10] E. Kh. Akhmedov and J. Pulido, Phys. Lett. B **553**, 7 (2003).
[11] Z. Berezhiani *et al.*, JETP Lett. **55**, 151 (1992); A. Acker *et al.*, Phys. Lett. B **285**, 371 (1992); A. S. Joshipura *et al.*, Phys. Rev. D **66**, 113008 (2002); J. F. Beacom and N. F. Bell, Phys. Rev. D **65**, 113009 (2002); A. Bandyopadhyay *et al.*, Phys. Rev. D **63**, 113019 (2001).
[12] P. Vogel *et al.*, Phys. Rev. C **24**, 1543 (1981); A. A. Hahn *et al.*, Phys. Lett. B **218**, 365 (1989); K. Schreckenbach *et al.*, Phys. Lett. B **118**, 162 (1982).
[13] J. Boger *et al.*, Nucl. Instrum. Methods Phys. Res., Sect. A **449**, 172 (2000).
[14] C. E. Ortiz *et al.*, Phys. Rev. Lett. **85**, 2909 (2000).
[15] J. N. Bahcall *et al.*, Astrophys. J. **555**, 990 (2001).
[16] S. Nakamura *et al.*, Nucl. Phys. **A707**, 561 (2002).
[17] T. Gaisser *et al.*, Phys. Rev. D **39**, 3532 (1989); T. Gaisser *et al.*, Phys. Rev. D **38**, 85 (1988).
[18] We would like to thank the U.S. Nuclear Regulatory Commission and AECL Chalk River Laboratories for providing this information.
[19] K. Schreckenbach *et al.*, Phys. Lett. **160B**, 325 (1985); K. Schreckenbach *et al.*, Phys. Lett. B **218**, 365 (1989).
[20] S. Ando *et al.*, Astropart. Phys. **18**, 307 (2003).
[21] M. Malek *et al.*, Phys. Rev. Lett. **90**, 061 101 (2003).
[22] D. Casper, Nucl. Phys. B Proc. Suppl. **B112**, 161 (2002).
[23] The number quoted in [6] is smaller by a factor of 4 but cannot be used here because it represents (g U *equivalent*)/(g D_2O), which assumes equilibrium in the ^{238}U decay chain. However, the equilibrium in the ^{238}U decay chain is broken as a result of radiochemical assays and due to the introduction of radon to the experiment. We thank L. Yang and R. Sturgeon of the National Research Council of Canada for this measurement.
[24] J. Terrell, Phys. Rev. **108**, 783 (1957).
[25] S. Eidelman *et al.*, Phys. Lett. B **592**, 1 (2004).
[26] Y. Gando *et al.*, Phys. Rev. Lett. **90**, 171 302 (2003).
[27] G. J. Feldman and R. D. Cousins, Phys. Rev. D **57**, 3873 (1998).
[28] J. Conway and K. Maeshima, http://fnth37.fnal.gov/higgs/poisson.ps; J. Conrad *et al.*, Phys. Rev. D **67**, 012002 (2003); G. C. Hill, Phys. Rev. D **67**, 118101 (2003).
[29] K. Eguchi *et al.*, Phys. Rev. Lett. **92**, 071 301 (2004).
[30] M. Aglietta *et al.*, JETP Lett. **63**, 791 (1996).
[31] K. Inoue, Ph.D, thesis University of Tokyo, 1993.
[32] We thank S. Pakvasa and J. Busenitz for valuable discussions on neutrino decay.